27. C. Costello, S. D. Gaines, J. Lynham, *Science* **321**, 1678–1681 (2008).
28. N. L. Gutiérrez, R. Hilborn, O. Defeo, *Nature* **470**, 386–389 (2011).

ACKNOWLEDGMENTS

We thank M. Arseneau, L. Grant, H. Kobluk, J. Nelson, and S. Leaver for data collection; L. Reshitnyk for creating fig. S1; and P. Ehlers and J. Ehlers for statistical assistance. S. Anderson, J. Baum, T. Branch, J. Brashares, A. Calestagne, S. Carlson, T. Davies, D. Kramer, T. Levi, J. Reynolds, and the "Ecology@UVic" discussion group offered insight on drafts. We thank the Raincoast Conservation, Tula, Wilburforce, and Willowgrove Foundations. C.T.D. and T.E.R. acknowledge Natural Sciences and Engineering Research Council of Canada Discovery Grant 435683 and National Research Council Canada Operating Grant 2354, respectively. Data and R code available in Dryad (doi:10.5061/dryad.238b2). T.E.R. conceived of the idea and created the preliminary data set. C.T.D., H.M.B., C.H.F., and T.E.R. designed the research. C.T.D. led data collection and project management. H.M.B., C.T.D., and C.H.F. conducted analyses. C.T.D., C.H.F., H.M.B., and T.E.R. wrote the manuscript.

SUPPLEMENTARY MATERIALS

www.sciencemag.org/content/349/6250/858/suppl/DC1
Materials and Methods
Supplementary Text
Figs. S1 to S6
Tables S1 to S2
References (*29*, *30*)

24 April 2015; accepted 13 July 2015
10.1126/science.aac4249

PLANT MICROBIOME

Salicylic acid modulates colonization of the root microbiome by specific bacterial taxa

Sarah L. Lebeis,[1,2]*† Sur Herrera Paredes,[2,3,4]† Derek S. Lundberg,[2,5]†‡ Natalie Breakfield,[2]§ Jase Gehring,[2]‖ Meredith McDonald,[2] Stephanie Malfatti,[6]¶ Tijana Glavina del Rio,[6] Corbin D. Jones,[2,4,5,7] Susannah G. Tringe,[6] Jeffery L. Dangl[2,3,4,5,7,8]*

Immune systems distinguish "self" from "nonself" to maintain homeostasis and must differentially gate access to allow colonization by potentially beneficial, nonpathogenic microbes. Plant roots grow within extremely diverse soil microbial communities but assemble a taxonomically limited root-associated microbiome. We grew isogenic *Arabidopsis thaliana* mutants with altered immune systems in a wild soil and also in recolonization experiments with a synthetic bacterial community. We established that biosynthesis of, and signaling dependent on, the foliar defense phytohormone salicylic acid is required to assemble a normal root microbiome. Salicylic acid modulates colonization of the root by specific bacterial families. Thus, plant immune signaling drives selection from the available microbial communities to sculpt the root microbiome.

Recognition of plant pathogens in leaves leads to dramatic changes in transcription, synthesis of defense phytohormones and antimicrobial compounds, and elaboration of physical barriers (*1*, *2*). Defense phytohormones are structurally diverse plant secondary metabolites that integrate plant immune system output responses while repressing cell growth and proliferation. Salicylic acid (SA), jasmonic acid (JA), and gaseous ethylene mediate localized and systemic plant immune responses (*3*, *4*). Nonspecific systemic acquired resistance is mediated by SA in leaves (*5*). In contrast, induced systemic resistance in leaves can be triggered by specific rhizobacteria colonizing roots and is mediated by JA and ethylene (*4*). SA and JA act antagonistically in responses to infection by biotrophs, at least in leaves (*6*). The defense phytohormones control a set of overlapping signaling sectors, each contributing to the regulation of plant defense via transcriptional and biosynthetic output in leaves (*7*).

Accessions of *Arabidopsis thaliana* show variation in defense phytohormone profiles after infection, even though they share similar root-associated bacterial microbiota (*8*–*10*). Previous studies examined the roles of defense phytohormones in shaping the wild-type root microbiome by using single mutant lines defective in their biosynthesis or perception, or exogenous defense hormone application in combination with bacterial culturing and/or lower-resolution profiling methods. No generalizable clarity has emerged to date (*11*, *12*). We therefore compared the bacterial root microbiome of wild-type *A. thaliana* accession Col-0 with a set of isogenic mutants lacking biosynthesis of, and/or signaling dependent on, at least one of the following: SA, JA, and ethylene. We focused on those with multiple mutations that eliminated overlapping defense-signaling sectors (Fig. 1A and table S1) (*13*). We anticipated that this experimental design would reveal the contributions of plant defense phytohormones to wild-type root microbiome composition.

Through sequencing the 16*S* rRNA gene, we profiled bacterial communities of rhizosphere (soil directly adjacent to the root) and endophytic compartment (EC) from roots grown in a previously characterized wild soil from the University of North Carolina Mason Farm biological preserve, as well as unplanted bulk soil (figs. S1 to S4, tables S2 to S4, and supplementary materials, materials and methods 1 to 3 and 6a to 6d) (*10*). Sample fraction (soil, rhizosphere, or endophytic compartment) and the differentiation of endophytic samples from bulk soil and rhizosphere explained the largest proportions of variance across the bacterial communities examined (table S5) (*8*, *10*). Endophytic bacterial communities were less diverse than bulk soil and rhizosphere communities (Fig. 1B and fig. S4), with reduced representation of Acidobacteria, Bacteroidetes, and Verrucomicrobia and enrichment of Actinobacteria and Firmicutes [analysis of variance (ANOVA), q value < 0.05]. Individual Proteobacteria families were either enriched or depleted in endophytic communities as compared with those of bulk soil and rhizosphere samples (fig. S5 and supplementary materials, materials and methods 6b). These results are consistent with distributions of bacterial phyla from *A. thaliana* roots grown in four wild soils (*8*, *10*).

Plant genotype affected phylum-level bacterial root endophytic community composition [4.3 to 5.0%, canonical analysis of principal coordinates (CAP)] (Fig. 1B and supplementary materials, materials and methods 4b and 6e) (*14*), with both hyperimmune *cpr5* and immunocompromised quadruple *dde1 ein2 pad4 sid2* mutant communities displaying lower α-diversity indices than that of the wild type (Fig. 1B, fig. S4B, and supplementary materials, materials and methods 1b). The relative abundance of Firmicutes was lower in immunocompromised *jar1 ein2 npr1*, *ein2 npr1*, and *npr1 jar1* mutants, which all lack response to SA (Fig. 1, A and B, and table S1). Actinobacteria were less abundant in *cpr5* and *pad4* endophytic samples, whereas Proteobacteria were more abundant in *cpr5* and *jar1 ein2 npr1* (Fig. 1, A and B; fig. S8; and supplementary materials, materials and methods 4a). Only mutants that lacked all

[1]Department of Microbiology, University of Tennessee, Knoxville, TN 37996-0845, USA. [2]Department of Biology, University of North Carolina, Chapel Hill, NC 27599-3280, USA. [3]Howard Hughes Medical Institute, University of North Carolina, Chapel Hill, NC 27599-3280, USA. [4]Curriculum in Bioinformatics and Computational Biology, University of North Carolina, Chapel Hill, NC 27599-3280, USA. [5]Curriculum in Genetics and Molecular Biology, University of North Carolina, Chapel Hill, NC 27599-3280, USA. [6]Joint Genome Institute, U.S. Department of Energy, Walnut Creek, CA, USA. [7]Carolina Center for Genome Sciences, University of North Carolina, Chapel Hill, NC 27599-3280, USA. [8]Department of Microbiology and Immunology, University of North Carolina, Chapel Hill, NC 27599-3280, USA.
***Corresponding author. E-mail: slebeis@utk.edu (S.L.L.); dangl@email.unc.edu (J.L.D.)** †These authors contributed equally to this work. ‡Present address: Department of Molecular Biology, Max Planck Institute for Developmental Biology, 72076 Tübingen, Germany. §Present address: NewLeaf Symbiotics, St. Louis, MO 63132, USA. ‖Present address: Department of Molecular and Cell Biology, University of California, Berkeley, Berkeley, CA 94720, USA. ¶Present address: Lawrence Livermore National Laboratory, Livermore, CA 94550-9234, USA.

three defense hormone signaling systems exhibited diminished survival that correlated with the presence of an unidentified oomycete in the root microbiota of survivors (fig. S2 and supplementary materials, materials and methods 3g).

We identified, using a zero inflated negative binomial (ZINB) model, bacterial families and operational taxonomic units (OTUs) in the root endophyte microbiome of each mutant plant line that were differentially abundant as compared with wild-type plants (tables S6 and S7, fig. S9, and supplementary materials, materials and methods 6b). Both the number of differentially abundant bacterial taxa and their identity differed in endophytic samples from mutants. Among 52 differentially abundant families in surviving *dde1 ein2 pad4 sid2* mutant endophytic samples, nearly all were depletions (Fig. 1C and fig. S6), which is consistent with this mutant's decreased α-diversity (Fig. 1B). Differentially abundant bacterial families were consistent with the significant relative phyla differences observed in specific defense hormone mutants (Fig. 1B and fig. S6A). In *cpr5*, for example, nine Actinobacteria families were identified with decreased relative abundance, and 12 Proteobacteria families were identified with increased relative abundance, in comparison with wild type (Fig. 1C, fig. S5, and table S6). These differences demonstrate that defense phytohormones modulate root microbiome composition at multiple taxonomic levels from phylum to family.

We then compared the enrichment and depletion profiles across the mutant genotypes in order to identify shared patterns (fig. S6C and supplementary materials, materials and methods 6d). Two striking genotype groups were observed (Fig. 1C). Group 1 mutants constitutively produce and accumulate SA, whereas group 2 mutants either accumulate less SA or cannot respond to it. These two genotype groups exhibited complementary patterns of differentially abundant Proteobacteria: In group 1, these were α- and β-Proteobacteria, whereas in group 2, they were γ-Proteobacteria (table S6 and fig. S6A). Within genotype group 2, nearly all of the differentially abundant bacterial families in *sid2* were shared with *pad4* and *dde1 ein2 pad4 sid2*, especially those families depleted as compared with the wild type. Half of the *dde1 ein2 pad4 sid2* depletions were apparently SA-independent (Fig. 1D and fig. S6B).

We reanalyzed the data to ask whether the differential family abundances observed in specific mutant groups remained consistent at higher taxonomic (OTU) resolution (table S4, tab B; table S7; and supplementary materials, materials and methods 6b). We largely recapitulated mutant groups 1 and 2 at OTU resolution (fig. S7B). If the plant selected bacteria at a low (genus or species) taxonomic level, we would expect that only one or a few abundant OTUs would drive, and thus correlate with, family-level analyses. However, we observed that a number of OTUs from across the abundance range matched family-level enrichment profiles (fig. S7, C to F, and supplementary materials, materials and methods 6b). These results suggest that defense phytohormones, particularly SA, modulate taxonomic groups of bacteria at the family level in the root, and not by altering the abundance of a small number of dominant strains within each differentially abundant family.

We next asked whether the bacterial families affected by the plant defense phytohormone mutants corresponded to taxa that were normally either enriched or depleted in wild-type roots compared with bulk soil. We resequenced two regions of the 16*S* gene across a subset of the samples using a different technology. This allowed us to eliminate sequencing and amplification biases. We identified 19 enriched and 23 depleted families in endophytic samples of wild-type roots compared with soil (table S8, fig. S11, and supplementary materials, materials and methods 6c). Consistent with phyla-level analyses (Fig. 1B), 79% of the bacterial families enriched in endophytic samples were Actinobacteria or Proteobacteria. Further, 55% of the endophytic-enriched families in SA mutants are Actinobacteria or Proteobacteria (tables S6 and S8). A similar pattern was observed in the OTU-level analysis, in which 42 and 48% of the endophytic-enriched bacterial families contained at least one OTU that is further enriched in the phytohormone mutants (tables S7 and S8).

Six of the 19 endophytic-enriched families (table S8) were depleted in the *cpr5* mutant that constitutively produces SA (table S6), suggesting that these six bacterial families are sensitive to SA or SA-dependent processes. Five different endophytic-enriched families (table S8) were further enriched in group 2 mutants that lack SA biosynthesis and signaling (table S6). Thus, these five bacterial families are candidates for taxa whose colonization is normally limited by wild-type levels of SA and/or SA-dependent processes. In contrast, 12 of the 23 endophytic-depleted families (table S8) were further depleted in group 2 mutants but not in group 1 mutants. Hence, these endophytic-depleted families may require SA-dependent processes to maintain even their very low abundance in the wild-type endophytic compartment (tables S6 and S8). Thus, SA is required to modulate the assembly of a normal root microbiome. In its absence, core root bacterial community composition is substantially

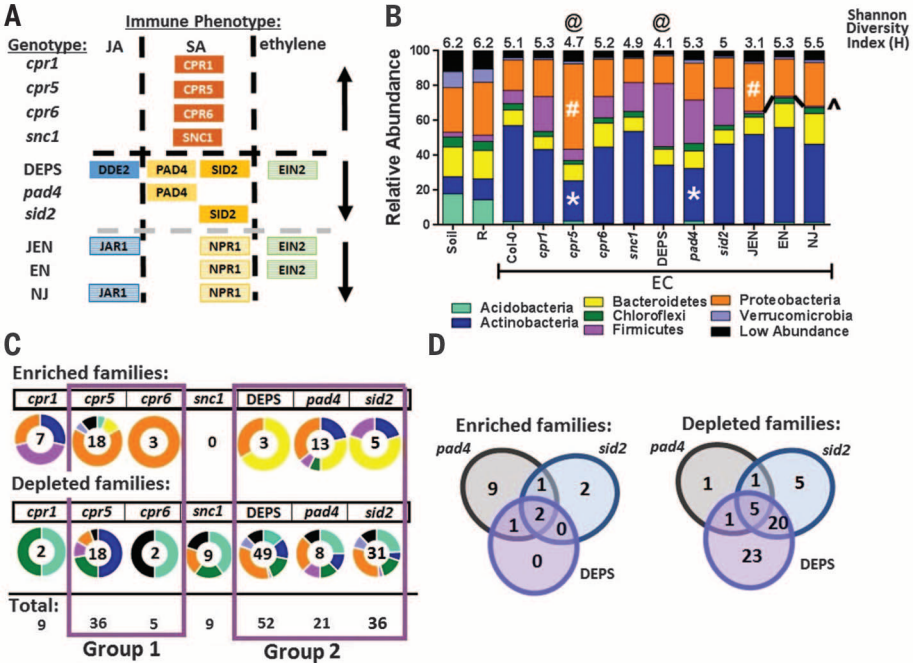

Fig. 1. Defense phytohormone mutants have altered root bacterial communities compared with those of wild-type plants. (**A**) JA, SA, and ethylene mutants (names at left) derived from wild-type Col-0. Upward and downward black arrows at right indicate hyper- and hypo-immune mutants, respectively. (**B**) Phyla distributions were separated into sample fractions [soil, Col-0 rhizosphere (R), or EC] and plant genotypes. Shannon diversity indices are listed above each bar. Asterisk indicates a phylum significantly lower than Col-0 EC at $P < 0.001$; pound sign indicates a phylum significantly higher than Col-0 EC at $P < 0.05$; and caret indicates that JEN, EN, and NJ Firmicutes relative abundances were significantly lower than Col-0 EC at $P < 0.04$; "@" indicates that the Shannon diversity index is significantly lower than Col-0 EC at $P < 0.001$ (all ANOVA with post hoc Tukey test). (**C**) The phyla distribution [circles color-coded as in (B)] of bacterial families identified as either enriched or depleted in ECs of each mutant compared with Col-0. The number of families in each category is noted inside each donut. Groups defined by means of Monte Carlo testing of Manhattan distances. (**D**) Venn diagrams showing the overlap of (left) enriched or (right) depleted group 2 families from (B).

altered. However, these changes to the bacterial microbiome are not sufficient to alter survival of these mutants in this particular wild soil.

We asked whether bacteria isolated from roots can colonize sterile roots in the context of a defined but complex synthetic bacterial community. We planted sterile seedlings (wild type and defense phytohormone mutants) in a calcined clay substrate inoculated with a synthetic community (SynCom) of bacteria (supplementary materials, materials and methods 5). Sixteen SynCom strains (table S9) were members of 10 families enriched in endophytic compartments of wild-type plants as compared with soil (table S8), and 18 strains matched family OTUs altered in plant defense hormone mutants (tables S6 and S9). Further, 21 of the 38 strains belonged to families that matched endophytic-enriched OTUs from a published census of plants grown in wild Mason Farm soil (*10*).

Both bulk soil and endophytic compartment microbiomes changed over 8 weeks after SynCom inoculation (Fig. 2A). Fourteen of the 38 SynCom strains were "robust colonizers" (fig. S13C, table S9, and supplementary materials, materials and methods 6h). Six of these 14 are from families predicted to be endophytic-enriched in roots from our Mason Farm soil census (Fig. 2B, overlapping black and orange circles, and table S9), corroborating their ability to colonize roots. We identified six "SynCom EC-enriched" isolates and eight "SynCom EC-depleted" isolates (Fig. 2C, table S4e, and supplementary materials, materials and methods 6f). Five of the six SynCom EC-enriched strains belong to families also predicted to be endophytic-enriched in roots from the Mason Farm soil census (Fig. 2B, overlapping orange and red circles, and table S9), supporting their categorization as endophytic compartment–enriched families (table S8). Thus, (i) some but not all SynCom isolates robustly colonized the endophytic compartment of host plants in these mesocosms, (ii) the soil and endophytic microbiomes still differed in this context, and (iii) there was considerable overlap in enrichments and depletions between the SynCom and wild soil colonization experimental platforms at the family level.

Seven bacterial isolates were differentially abundant between wild type and the defense phytohormone mutants in the SynCom experiments (Fig. 3 and supplementary materials, materials and methods 6f), including at least one representative from each of the four phyla present in the inoculum (table S9). Six of the seven isolates were either depleted (*Streptomyces* sp. 136, *Chryseobacterium* sp. 8, *Pseudomonas* sp. 50, and *Escherichia coli*) or were sporadic or non-colonizers (*Bacillus* sp. 125 and *Brevundimonas* sp. 374). Four of these six overlapped with families predicted to be differentially abundant across genotypes in our Mason Farm soil census (Fig. 3B and table S6), and six of seven (all except *Bacillus* sp. 125) were enriched in the defense phytohormone mutants (Fig. 3C). The profiles of differentially abundant isolates in *pad4* and *sid2* mutants overlapped (Fig. 3C). These data integrate our SynCom experiments with our wild soil census and demonstrate increased abundance in the SA-deficient mutants of isolates that were "sporadic or non-colonizers" across all wild soil endophytic samples. Thus, altering SA production and signaling in the host plant prevents it from fully excluding bacterial taxa that a wild-type plant shuns.

Exogenous SA application to our SynCom experiments also affected bacterial community composition in both bulk soil and endophytic compartment samples (CAP 0.3 to 1.5%) (fig. S14A, table S5, and supplementary materials, materials and methods 5b and 6e), which is consistent with rhizosphere changes in plants treated with SA or JA (*15*, *16*). Two isolates were enriched [*Flavobacterium* sp. 40 (Bacteroidetes) and *Terracoccus* sp. 273 (Actinobacteria)] and one depleted [*Mitsuaria* sp. 370 (β-Proteobacteria)] in the presence of exogenous SA (table S9; fig. S14, B and C; and supplementary materials, materials and methods 6f). *Terracoccus* sp. 273 abundance was higher in both SA-treated bulk soil and root endophytic samples (Fig. 4A), and its growth was enhanced by SA in liquid media (Fig. 4B and supplementary materials, materials and methods 5c), although its genome contains no obvious SA catabolism genes (taxon IDs in table S9). In contrast, *Mitsuaria* sp. 370 was depleted in endophytic

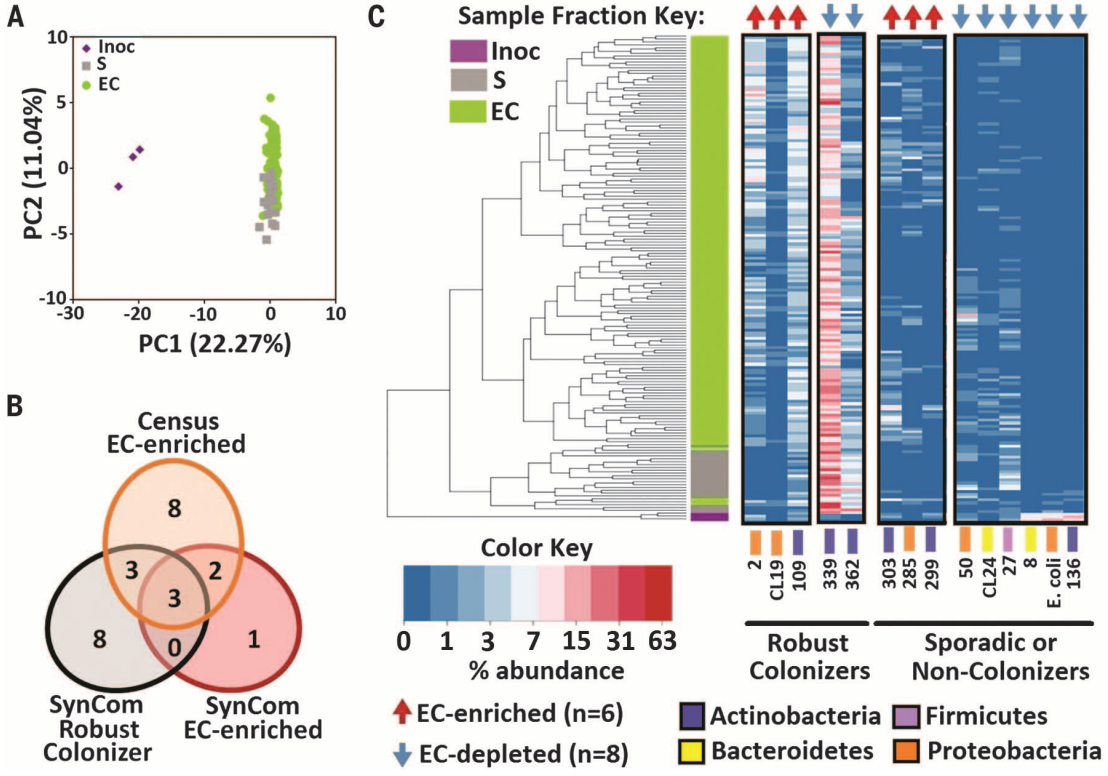

Fig. 2. A 38-member synthetic community recapitulates differentiated microbiome colonization. (**A**) Principal coordinates analysis showing the inoculum (purple diamonds), soil (gray squares), and EC (green circles) samples. (**B**) The overlap of SynCom members that were robust colonizers of Col-0 EC (black), EC-enriched (red), or matched EC-enriched families from the census of roots grown in wild Mason Farm soil (orange) (Fig. 1). (**C**) Hierarchical clustering and heat map showing percent abundance (log_2 scale) of selected isolates. Sample clustering splits by fraction (left) and EC samples grouping by biological replicate. Isolates are grouped by their presence in the majority of Col-0 EC samples (Robust colonizers) or absence in the majority of Col-0 EC samples (sporadic or non-colonizers). Isolates are color-coded to phyla as in Fig. 1. Isolates that were significantly more abundant (red arrows) or less abundant (blue arrows) in EC with respect to bulk soil are denoted along the top.

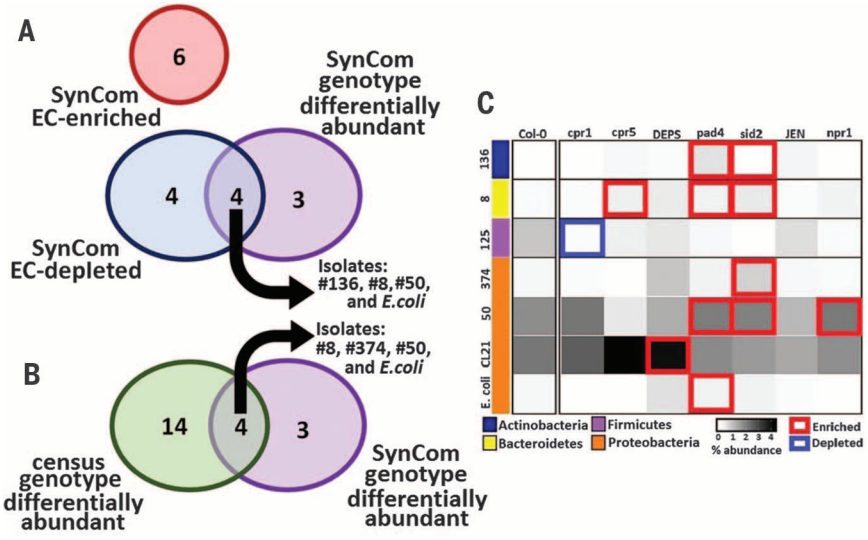

Fig. 3. Defense phytohormone mutants exhibit increased abundance of EC-depleted microbes. (**A**) Overlap of SynCom EC-depleted (Fig. 2C) and SynCom isolates differentially abundant in defense phytohormone mutants (SynCom genotype differentially abundant). No SynCom EC-enriched isolates (Fig. 2, B and C) were affected by plant genotype. (**B**) Overlap of the same SynCom genotype differentially abundant isolates from (A) compared with isolates present in the SynCom from families that were genotype differentially abundant in the wild soil census (green circle) (table S8). (**C**) Heat map of isolates (color-coded by phylum as in Fig. 1) differentially abundant between defense phytohormone mutants and Col-0. Grayscale shows the mean abundance of the corresponding isolate (rows) in the EC of a given genotype (columns). Genotype differentially abundant families predicted as enriched or depleted by the ZINB model are boxed in red or blue, respectively (supplementary materials, materials and methods 6f).

samples treated with SA and grew less well in its presence (Fig. 4, C and D). *Streptomyces* sp. 303 was weakly enriched in SA-treated samples (q value <0.07) (Fig. 4E), grew on minimal media with 0.5 mM SA as a sole carbon source (Fig. 4F), and contains orthologs to a previously characterized *Streptomyces* SA-degradation operon (fig. S14D and table S9). Thus, the broader effects of SA on microbiome composition consist of both direct and indirect effects on the physiologies of individual community members from limited, specific taxa.

We demonstrate that plant defense phytohormones sculpt the root microbiome in characteristic ways. Elimination of all three defense phytohormone signaling sectors results in abnormal microbial profiles in the root, which may be linked to lowered survival in a wild soil. SA, a key immune regulator in leaves, also modulates the composition of the root microbiome. Plants with altered SA signaling have root microbiomes that differ in the relative abundance of specific bacterial families as compared with those of wild type. It will be of interest to address whether and how the extra- and intracellular plant immune system receptor systems further condition root bacterial community composition. We demonstrated that different bacterial strains could make use of SA in different ways, whether as a growth signal or as a carbon source. Thus, SA influences the microbial community structure of the root. This may occur by gating bacterial taxa as a consequence of SA function in homeostatic control of immune system outputs, or via as-yet-undefined effects on microbe-microbe interactions and root physiology. Together, our results show that a

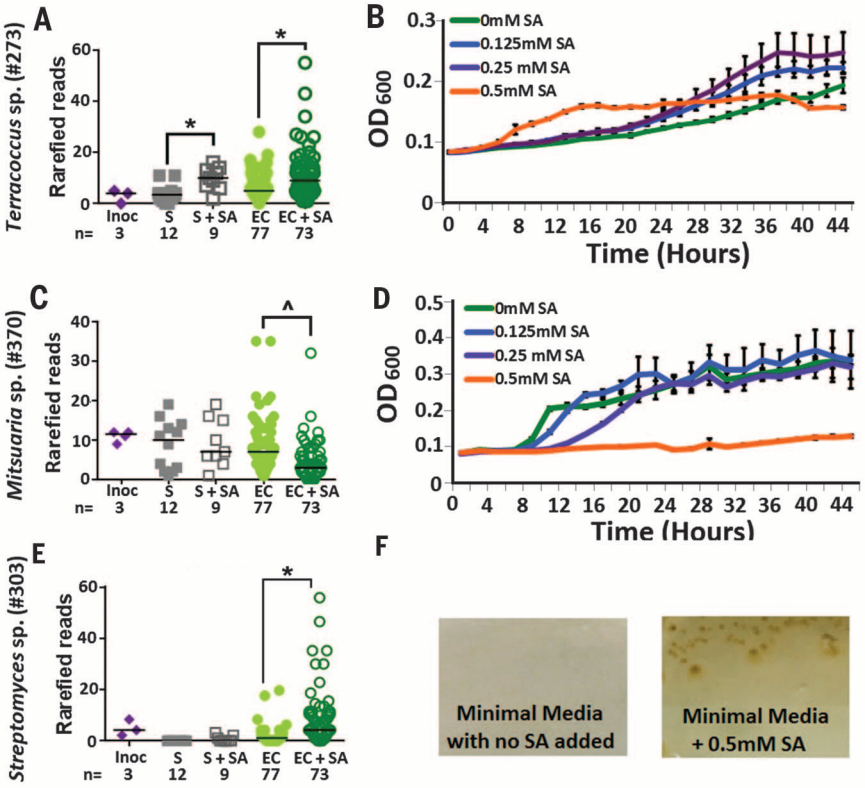

Fig. 4. SA directly affects synthetic community isolates. (**A**) *Terracoccus* sp. (273) reads from 400 rarefied consensus sequences for the synthetic community inoculum (purple diamonds), soil (gray squares), and EC samples (green circles) from SA-treated (open symbols) and -untreated (closed symbols) plants. Asterisk indicates significantly different between sample treatments at $P < 0.006$ by Mann-Whitney test. (**B**) Optical density of *Terracoccus* sp. (273) grown in buffered 1/10 LB with 0 (green), 0.125 (blue), 0.25 (purple), or 0.5 mM (orange) SA added. (**C**) *Mitsuaria* sp. (370) reads as in (A). Caret indicates significantly different between EC sample treatments at $P < 0.0001$ by means of Mann-Whitney test. (**D**) Optical density of *Mitsuaria* sp. (370) grown as in (B). (**E**) *Streptomyces* sp. (303) reads. Asterisk indicates significantly different between EC sample treatments at $P < 0.001$ by means of Mann-Whitney test. (**F**) *Streptomyces* sp. (303) aggregates in liquid cultures but grows on minimal media agar with 0.5 mM SA as the sole carbon source.

central regulator of the plant immune system, largely uncharacterized in the root, directly influences root microbiome composition. Our results could open new avenues for modulating the root microbiome to enhance crop production and sustainability.

Note added in proof: Figure 1 was revised since this paper's original publication in *Science* Express.

REFERENCES AND NOTES

1. P. N. Dodds, J. P. Rathjen, *Nat. Rev. Genet.* **11**, 539–548 (2010).
2. J. D. Jones, J. L. Dangl, *Nature* **444**, 323–329 (2006).
3. Y. Belkhadir, L. Yang, J. Hetzel, J. L. Dangl, J. Chory, *Trends Biochem. Sci.* **39**, 447–456 (2014).
4. C. M. Pieterse, D. Van der Does, C. Zamioudis, A. Leon-Reyes, S. C. Van Wees, *Annu. Rev. Cell Dev. Biol.* **28**, 489–521 (2012).
5. Z. Q. Fu, X. Dong, *Annu. Rev. Plant Biol.* **64**, 839–863 (2013).
6. B. Huot, J. Yao, B. L. Montgomery, S. Y. He, *Mol. Plant* **7**, 1267–1287 (2014).
7. Y. Kim *et al*., *Cell Host Microbe* **15**, 84–94 (2014).
8. D. Bulgarelli *et al*., *Nature* **488**, 91–95 (2012).
9. D. J. Kliebenstein, A. Figuth, T. Mitchell-Olds, *Genetics* **161**, 1685–1696 (2002).
10. D. S. Lundberg *et al*., *Nature* **488**, 86–90 (2012).
11. P. A. Bakker, R. L. Berendsen, R. F. Doornbos, P. C. Wintermans, C. M. Pieterse, *Front. Plant Sci.* **4**, 165 (2013).
12. R. Mendes, P. Garbeva, J. M. Raaijmakers, *FEMS Microbiol. Rev.* **37**, 634–663 (2013).
13. F. Katagiri, K. Tsuda, *Mol. Plant Microbe Interact.* **23**, 1531–1536 (2010).
14. M. J. Anderson, T. J. Willis, *Ecology* **84**, 511–525 (2003).
15. L. C. Carvalhais, P. G. Dennis, P. M. Schenk, *Appl. Soil Ecol.* **84**, 1–5 (2014).
16. R. F. Doornbos, B. P. Geraats, E. E. Kuramae, L. C. Van Loon, P. A. Bakker, *Mol. Plant Microbe Interact.* **24**, 395–407 (2011).

ACKNOWLEDGMENTS

This work was supported by NSF Microbial Systems Biology grant IOS-0958245 and NSF INSPIRE grant IOS-1343020 to J.L.D. S.H.P. was supported by NIH Training Grant T32 GM067553-06 and is a Howard Hughes Medical Institute (HHMI) International Student Research Fellow. D.S.L. was supported by NIH Training Grant T32 GM07092-34. J.L.D. is an Investigator of HHMI, supported by HHMI and the Gordon and Betty Moore Foundation (GBMF3030). S.L.L. was supported by the NIH Minority Opportunities in Research division of the National Institute of General Medical Sciences (NIGMS) grant K12GM000678. N.B. was supported by NIH Dr. Ruth L. Kirschstein National Research Service Award Fellowship F32-GM103156. The work conducted by the U.S. Department of Energy (DOE) Joint Genome Institute (JGI), a DOE Office of Science User Facility, is supported by the Office of Science of the DOE under contract DE-AC02-05CH11231. This work was also funded by the DOE–JGI Director's Discretionary Grand Challenge Program. We thank the Dangl laboratory microbiome group for useful discussions and S. Grant, S. Y. He, P. Hugenholtz, J. Kremer, and D. Weigel for critical comments on the manuscript. The supplementary materials contain additional data. J.L.D. is a cofounder, shareholder, and chair of the Scientific Advisory Board of AgBiome, a corporation whose goal is to use plant-associated microbes to improve plant productivity. Raw sequence data are available at the Short Read Archive accessions ERP010780 and ERP010863 and at the JGI portal http://genome.jgi.doe.gov/Immunesamples/Immunesamples.info.html, which requires registration to access.

SUPPLEMENTARY MATERIALS

www.sciencemag.org/content/349/6250/860/suppl/DC1
Materials and Methods
SupplementaryText
Figs. S1 to S14
References (*17*–*63*)
Tables S1 to S10
Databases S1 to S4

8 February 2015; accepted 26 June 2015
Published online 16 July 2015
10.1126/science.aaa8764

PARASITIC PLANTS

Probing strigolactone receptors in *Striga hermonthica* with fluorescence

Yuichiro Tsuchiya,[1,3]*† Masahiko Yoshimura,[1,2]† Yoshikatsu Sato,[1] Keiko Kuwata,[1] Shigeo Toh,[3] Duncan Holbrook-Smith,[3] Hua Zhang,[1] Peter McCourt,[3] Kenichiro Itami,[1,2,4] Toshinori Kinoshita,[1,2] Shinya Hagihara[1,2]*

Elucidating the signaling mechanism of strigolactones has been the key to controlling the devastating problem caused by the parasitic plant *Striga hermonthica*. To overcome the genetic intractability that has previously interfered with identification of the strigolactone receptor, we developed a fluorescence turn-on probe, Yoshimulactone Green (YLG), which activates strigolactone signaling and illuminates signal perception by the strigolactone receptors. Here we describe how strigolactones bind to and act via *ShHTL*s, the diverged family of α/β hydrolase-fold proteins in *Striga*. Live imaging using YLGs revealed that a dynamic wavelike propagation of strigolactone perception wakes up *Striga* seeds. We conclude that *ShHTL*s function as the strigolactone receptors mediating seed germination in *Striga*. Our findings enable access to strigolactone receptors and observation of the regulatory dynamics for strigolactone signal transduction in *Striga*.

Damages caused by the parasitic plant *Striga hermonthica* threaten food security in Africa. Infection of harvests by *Striga* leads to the loss of $10 billion U.S. dollars' worth of crops from the continent every year (*1*). Strigol and related strigolactones (*2*, *3*) derived from the host plants stimulate the germination of *Striga* by regulating the biosynthesis of plant hormones, including abscisic acid, gibberellins, and ethylene (*4*–*6*). So far, 17 strigolactones have been identified, which are unique according to the plant species (*7*–*9*). *Striga* recognizes host plants by sensing their particular strigolactone composition (*10*). However, the mechanism of how *Striga* senses minute amounts of structurally diverse strigolactones to identify their host targets remains unclear. Here we report the identification of the strigolactone receptor in *Striga*.

Strigolactones also function as plant hormones and as ecological signals for communicating with microbes (*11*–*13*). Genetic studies in model plants, including rice, *Arabidopsis*, and petunia, have led to identification of a group of α/β hydrolase-fold proteins as presumptive receptors for strigolactones (*14*–*17*). The unidentified strigolactone receptor in *Striga* may have a similar ligand selectivity to AtDWARF14 (AtD14), the strigolactone receptor in *Arabidopsis*, because AtD14 is also known to perceive natural and synthetic stimulants for *Striga* germination (*16*–*19*). However, *AtD14* regulates plant architecture, including shoot branching and root development, that has no obvious resemblance to *Striga* germination (*20*, *21*). In contrast, its homolog, *HYPOSENSITIVE TO LIGHT* (*AtHTL*)/*KARRIKIN INSENSITIVE2* (*KAI2*) is involved in seed germination stimulated by smoke-derived karrikins, a collection of imide-based agonists and non-natural stereoisomers of strigolactones in *Arabidopsis* (*16*, *22*, *23*). Therefore, the strigolactone receptors in *Striga* may have a comparable role to *AtHTL*, with ligand preferences similar to those of *AtD14* (fig. S1). On the other hand, the signaling processes of these homologs are highly related. Both AtD14 and AtHTL are considered to share an F-box protein, MORE AXILLARY GROWTH2 (AtMAX2), which directs their specific negative regulators to undergo ubiquitin-dependent proteasomal degradation (*24*, *25*). The ortholog of *AtMAX2* in *Striga* (*ShMAX2*) plays a role in regulating shoot branching and seed germination when expressed in *Arabidopsis*, thus suggesting that the signaling processes involving the F-box protein are conserved in *Striga* (*26*). Altogether, we hypothesized that *Striga* carries orthologs of either *AtD14* or *AtHTL* that have acquired new functions during the evolution of parasitism to respond to natural strigolactones and stimulate germination.

Here we report the use of small-molecule tools to probe the function of strigolactone receptors. AtD14 hydrolyzes strigolactones into the ABC-ring and D-ring fragments during the signaling process (fig. S2) (*15*). We applied this reaction to

[1]Institute of Transformative Bio-Molecules (WPI-ITbM), Nagoya University, Furo-cho, Chikusa-ku, Nagoya 464-8602, Japan. [2]Graduate School of Science, Nagoya University, Furo-cho, Chikusa-ku, Nagoya 464-8602, Japan. [3]Department of Cell and Systems Biology, University of Toronto, 25 Willcocks Street, Toronto, Ontario M5S 3B2, Canada. [4]Japan Science and Technology Agency–Exploratory Research for Advanced Technology, Itami Molecular Nanocarbon Project, Nagoya University, Furo-cho, Chikusa-ku, Nagoya 464-8602, Japan.
***Corresponding author. E-mail: yuichiro@itbm.nagoya-u.ac.jp (Y.T.); hagi@itbm.nagoya-u.ac.jp (S.H.)** †These authors contributed equally to this work.

Salicylic acid modulates colonization of the root microbiome by specific bacterial taxa
Sarah L. Lebeis, Sur Herrera Paredes, Derek S. Lundberg, Natalie Breakfield, Jase Gehring, Meredith McDonald, Stephanie Malfatti, Tijana Glavina del Rio, Corbin D. Jones, Susannah G. Tringe and Jeffery L. Dangl (July 16, 2015)
Science **349** (6250), 860-864. [doi: 10.1126/science.aaa8764]
originally published online July 16, 2015

Editor's Summary

Immune signals shape root communities

To thwart microbial pathogens aboveground, the plant *Arabidopsis* turns on defensive signaling using salicylic acid. In *Arabidopsis* plants with modified immune systems, Lebeis *et al.* show that bacterial communities change in response to salicylic acid signaling in the root zone as well (see the Perspective by Haney and Ausubel). Abundance of some root-colonizing bacterial families increased at the expense of others, partly as a function of whether salicylic acid was used as an immune signal or as a carbon source for microbial growth.

Science, this issue p. 860; see also p. 788

Science (print ISSN 0036-8075; online ISSN 1095-9203) is published weekly, except the last week in December, by the American Association for the Advancement of Science, 1200 New York Avenue NW, Washington, DC 20005.